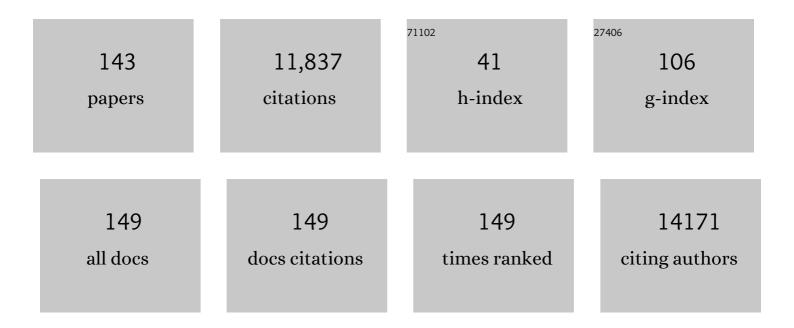
List of Publications by Year in descending order

Source: https://exaly.com/author-pdf/1941423/publications.pdf Version: 2024-02-01



ΡΛΙΙΙ \Ν/ ΒΟΗΝ

#	Article	IF	CITATIONS
1	Science and technology for water purification in the coming decades. Nature, 2008, 452, 301-310.	27.8	6,795
2	Gateable Nanofluidic Interconnects for Multilayered Microfluidic Separation Systems. Analytical Chemistry, 2003, 75, 1861-1867.	6.5	204
3	Nanofluidics in chemical analysis. Chemical Society Reviews, 2010, 39, 1060-1072.	38.1	168
4	In-plane control of morphology and tunable photoluminescence in porous silicon produced by metal-assisted electroless chemical etching. Journal of Applied Physics, 2002, 91, 6134-6140.	2.5	164
5	Temperature-Controlled Flow Switching in Nanocapillary Array Membranes Mediated by Poly(N-isopropylacrylamide) Polymer Brushes Grafted by Atom Transfer Radical Polymerization. Langmuir, 2007, 23, 305-311.	3.5	157
6	Manipulating Molecular Transport through Nanoporous Membranes by Control of Electrokinetic Flow:Â Effect of Surface Charge Density and Debye Length. Langmuir, 2001, 17, 6298-6303.	3.5	132
7	Miniaturized Lead Sensor Based on Lead-Specific DNAzyme in a Nanocapillary Interconnected Microfluidic Device. Environmental Science & Technology, 2005, 39, 3756-3761.	10.0	123
8	Immobilization of a Catalytic DNA Molecular Beacon on Au for Pb(II) Detection. Analytical Chemistry, 2005, 77, 442-448.	6.5	119
9	Science and technology for water purification in the coming decades. , 2009, , 337-346.		110
10	Hybrid three-dimensional nanofluidic/microfluidic devices using molecular gates. Sensors and Actuators A: Physical, 2003, 102, 223-233.	4.1	105
11	In-plane bandgap control in porous GaN through electroless wet chemical etching. Applied Physics Letters, 2002, 80, 980-982.	3.3	102
12	Nanocapillary Array Interconnects for Gated Analyte Injections and Electrophoretic Separations in Multilayer Microfluidic Architectures. Analytical Chemistry, 2003, 75, 2224-2230.	6.5	101
13	Redox Cycling in Nanoscale-Recessed Ring-Disk Electrode Arrays for Enhanced Electrochemical Sensitivity. ACS Nano, 2013, 7, 5483-5490.	14.6	99
14	Nanofluidics: Systems and Applications. IEEE Sensors Journal, 2008, 8, 441-450.	4.7	93
15	Induced Electrokinetic Transport in Microâ^'Nanofluidic Interconnect Devices. Langmuir, 2007, 23, 13209-13222.	3.5	89
16	MALDI-guided SIMS: Multiscale Imaging of Metabolites in Bacterial Biofilms. Analytical Chemistry, 2014, 86, 9139-9145.	6.5	79
17	Direct assay ofAplysia tissues and cells with laser desorption/ionization mass spectrometry on porous silicon. Journal of Mass Spectrometry, 2001, 36, 1317-1322.	1.6	73
18	Genetic engineering of surface attachment sites yields oriented protein monolayers. Journal of the American Chemical Society, 1992, 114, 9298-9299.	13.7	70

#	Article	IF	CITATIONS
19	Direct-write patterning of microstructured porous silicon arrays by focused-ion-beam Pt deposition and metal-assisted electroless etching. Journal of Applied Physics, 2004, 96, 6888-6894.	2.5	69
20	Structural and spectroscopic characterization of porous silicon carbide formed by Pt-assisted electroless chemical etching. Solid State Communications, 2003, 126, 245-250.	1.9	65
21	Incorporation of a DNAzyme into Au-coated nanocapillary array membranes with an internal standard for Pb(ii) sensing. Analyst, The, 2006, 131, 41-47.	3.5	65
22	Microfluidic Separation and Gateable Fraction Collection for Mass-Limited Samples. Analytical Chemistry, 2004, 76, 6419-6425.	6.5	63
23	Correlated mass spectrometry imaging and confocal Raman microscopy for studies of three-dimensional cell culture sections. Analyst, The, 2014, 139, 4578.	3.5	61
24	Nanoscale Control and Manipulation of Molecular Transport in Chemical Analysis. Annual Review of Analytical Chemistry, 2009, 2, 279-296.	5.4	60
25	Electrochromic Sensor for Multiplex Detection of Metabolites Enabled by Closed Bipolar Electrode Coupling. ACS Sensors, 2017, 2, 1020-1026.	7.8	59
26	Whole-Cell <i>Pseudomonas aeruginosa</i> Localized Surface Plasmon Resonance Aptasensor. Analytical Chemistry, 2018, 90, 2326-2332.	6.5	59
27	Correlated Imaging with C ₆₀ -SIMS and Confocal Raman Microscopy: Visualization of Cell-Scale Molecular Distributions in Bacterial Biofilms. Analytical Chemistry, 2014, 86, 10885-10891.	6.5	58
28	Multimodal chemical imaging of molecular messengers in emerging Pseudomonas aeruginosa bacterial communities. Analyst, The, 2015, 140, 6544-6552.	3.5	58
29	Correlated imaging – a grand challenge in chemical analysis. Analyst, The, 2013, 138, 1924.	3.5	56
30	Chemisorption and Chemical Reaction Effects on the Resistivity of Ultrathin Gold Films at the Liquidâ^'Solid Interface. Analytical Chemistry, 1999, 71, 119-125.	6.5	55
31	Modeling and Simulation of Ionic Currents in Three-Dimensional Microfluidic Devices with Nanofluidic Interconnects. Journal of Nanoparticle Research, 2005, 7, 507-516.	1.9	54
32	Fabrication of antireflective layers on silicon using metal-assisted chemical etching with in situ deposition of silver nanoparticle catalysts. Solar Energy Materials and Solar Cells, 2012, 103, 98-107.	6.2	52
33	Redox Cycling on Recessed Ring-Disk Nanoelectrode Arrays in the Absence of Supporting Electrolyte. Journal of the American Chemical Society, 2014, 136, 7225-7228.	13.7	52
34	Inâ^'Plane Resistivity of Ultrathin Gold Films:  A High Sensitivity, Molecularly Differentiated Probe of Mercaptan Chemisorption at the Liquidâ^'Metal Interface. Journal of the American Chemical Society, 1998, 120, 9969-9970.	13.7	51
35	Surface Adsorption and Transfer of Organomercaptans to Colloidal Gold and Direct Identification by Matrix Assisted Laser Desorption/Ionization Mass Spectrometry. Journal of the American Chemical Society, 2004, 126, 5920-5926.	13.7	50
36	Single Entity Electrochemistry in Nanopore Electrode Arrays: Ion Transport Meets Electron Transfer in Confined Geometries. Accounts of Chemical Research, 2020, 53, 719-728.	15.6	50

#	Article	IF	CITATIONS
37	Recessed Ring–Disk Nanoelectrode Arrays Integrated in Nanofluidic Structures for Selective Electrochemical Detection. Analytical Chemistry, 2013, 85, 9882-9888.	6.5	49
38	Profiling pH Gradients Across Nanocapillary Array Membranes Connecting Microfluidic Channels. Journal of the American Chemical Society, 2005, 127, 13928-13933.	13.7	48
39	A Carotenoid-Deficient Mutant in Pantoea sp. YR343, a Bacteria Isolated from the Rhizosphere of Populus deltoides, Is Defective in Root Colonization. Frontiers in Microbiology, 2016, 7, 491.	3.5	48
40	Nanopore Electrochemistry: A Nexus for Molecular Control of Electron Transfer Reactions. ACS Central Science, 2018, 4, 20-29.	11.3	48
41	Ion Accumulation and Migration Effects on Redox Cycling in Nanopore Electrode Arrays at Low Ionic Strength. ACS Nano, 2016, 10, 3658-3664.	14.6	47
42	Enhanced Mass Transport of Electroactive Species to Annular Nanoband Electrodes Embedded in Nanocapillary Array Membranes. Journal of the American Chemical Society, 2012, 134, 8617-8624.	13.7	46
43	Morphology evolution and luminescence properties of porous GaN generated via Pt-assisted electroless etching of hydride vapor phase epitaxy GaN on sapphire. Journal of Applied Physics, 2003, 94, 7526.	2.5	44
44	Nanocapillary Arrays Effect Mixing and Reaction in Multilayer Fluidic Structures. Angewandte Chemie - International Edition, 2004, 43, 1862-1865.	13.8	42
45	Surface Immobilization of Catalytic Beacons Based on Ratiometric Fluorescent DNAzyme Sensors:  A Systematic Study. Langmuir, 2007, 23, 9513-9521.	3.5	42
46	Monodisperse GaN nanowires prepared by metal-assisted chemical etching with in situ catalyst deposition. Electrochemistry Communications, 2012, 19, 39-42.	4.7	42
47	Spatial organization of Pseudomonas aeruginosa biofilms probed by combined matrix-assisted laser desorption ionization mass spectrometry and confocal Raman microscopy. Analyst, The, 2014, 139, 5700-5708.	3.5	42
48	Spatial Correlation of Confocal Raman Scattering and Secondary Ion Mass Spectrometric Molecular Images of Lignocellulosic Materials. Analytical Chemistry, 2010, 82, 2608-2611.	6.5	41
49	Single occupancy spectroelectrochemistry of freely diffusing flavin mononucleotide in zero-dimensional nanophotonic structures. Faraday Discussions, 2015, 184, 101-115.	3.2	41
50	Potential-dependent single molecule blinking dynamics for flavin adenine dinucleotide covalently immobilized in zero-mode waveguide array of working electrodes. Faraday Discussions, 2013, 164, 57.	3.2	39
51	Self-induced redox cycling coupled luminescence on nanopore recessed disk-multiscale bipolar electrodes. Chemical Science, 2015, 6, 3173-3179.	7.4	36
52	Coupling of Independent Electrochemical Reactions and Fluorescence at Closed Bipolar Interdigitated Electrode Arrays. ChemElectroChem, 2016, 3, 422-428.	3.4	36
53	Single-molecule spectroelectrochemical cross-correlation during redox cycling in recessed dual ring electrode zero-mode waveguides. Chemical Science, 2017, 8, 5345-5355.	7.4	36
54	Optical determination of surface density in oriented metalloprotein nanostructures. Analytical Chemistry, 1993, 65, 1635-1638.	6.5	35

#	Article	IF	CITATIONS
55	Metal-Assisted Chemical Etching Using Tollen's Reagent to Deposit Silver Nanoparticle Catalysts for Fabrication of Quasi-ordered Silicon Micro/Nanostructures. Journal of Electronic Materials, 2011, 40, 2480-2485.	2.2	35
56	Effect of Molecular Adsorption on the Electrical Conductance of Single Au Nanowires Fabricated by Electronâ€Beam Lithography and Focused Ion Beam Etching. Small, 2010, 6, 2598-2603.	10.0	34
57	Spatial Mapping of Pyocyanin in <i>Pseudomonas Aeruginosa</i> Bacterial Communities Using Surface Enhanced Raman Scattering. Applied Spectroscopy, 2017, 71, 215-223.	2.2	34
58	Voltage-Tunable Volume Transitions in Nanoscale Films of Poly(hydroxyethyl methacrylate) Surfaces Grafted onto Gold. Langmuir, 2005, 21, 1979-1985.	3.5	33
59	Spatially dependent alkyl quinolone signaling responses to antibiotics in Pseudomonas aeruginosa swarms. Journal of Biological Chemistry, 2018, 293, 9544-9552.	3.4	33
60	Closed bipolar electrode-enabled dual-cell electrochromic detectors for chemical sensing. Analyst, The, 2016, 141, 6018-6024.	3.5	31
61	Electrolysis in nanochannels for in situ reagent generation in confined geometries. Lab on A Chip, 2011, 11, 3634.	6.0	30
62	Redox Cycling in Nanopore-Confined Recessed Dual-Ring Electrode Arrays. Journal of Physical Chemistry C, 2016, 120, 20634-20641.	3.1	30
63	Raman chemical imaging of the rhizosphere bacterium Pantoea sp. YR343 and its co-culture with Arabidopsis thaliana. Analyst, The, 2016, 141, 2175-2182.	3.5	30
64	Quantitative SIMS Imaging of Agar-Based Microbial Communities. Analytical Chemistry, 2018, 90, 5654-5663.	6.5	30
65	Electrochemistry at single molecule occupancy in nanopore-confined recessed ring-disk electrode arrays. Faraday Discussions, 2016, 193, 51-64.	3.2	29
66	High sensitivity hydrogen sensing with Pt-decorated porous gallium nitride prepared by metal-assisted electroless etching. Analyst, The, 2010, 135, 902.	3.5	27
67	Real-time image denoising of mixed Poisson–Gaussian noise in fluorescence microscopy images using ImageJ. Optica, 2022, 9, 335.	9.3	27
68	Ion selective redox cycling in zero-dimensional nanopore electrode arrays at low ionic strength. Nanoscale, 2017, 9, 5164-5171.	5.6	26
69	Detection of 1†zmol injection of angiotensin using capillary zone electrophoresis coupled to a Q-Exactive HF mass spectrometer with an electrokinetically pumped sheath-flow electrospray interface. Talanta, 2019, 204, 70-73.	5.5	26
70	Single-Molecule Enzyme Dynamics of Monomeric Sarcosine Oxidase in a Gold-Based Zero-Mode Waveguide. Applied Spectroscopy, 2012, 66, 163-169.	2.2	24
71	Asymmetric Nafion-Coated Nanopore Electrode Arrays as Redox-Cycling-Based Electrochemical Diodes. ACS Nano, 2018, 12, 9177-9185.	14.6	24
72	Electrochemical Surface-Enhanced Raman Spectroscopy of Pyocyanin Secreted by <i>Pseudomonas aeruginosa</i> Communities. Langmuir, 2019, 35, 7043-7049.	3.5	24

#	Article	IF	CITATIONS
73	Interfacial Scattering at Electrochemically Fabricated Atom-Scale Junctions between Thin Gold Film Electrodes in a Microfluidic Channel. Analytical Chemistry, 2005, 77, 243-249.	6.5	23
74	Zero-mode waveguide nanophotonic structures for single molecule characterization. Journal Physics D: Applied Physics, 2018, 51, 193001.	2.8	22
75	Near-field photoluminescence of microcrystalline arsenic oxides produced in anodically processed gallium arsenide. Applied Physics Letters, 1999, 74, 1096-1098.	3.3	21
76	Catalyst and processing effects on metal-assisted chemical etching for the production of highly porous GaN. Semiconductor Science and Technology, 2013, 28, 065001.	2.0	21
77	Metal-assisted polyatomic SIMS and laser desorption/ionization for enhanced small molecule imaging of bacterial biofilms. Biointerphases, 2016, 11, 02A325.	1.6	21
78	Optical Biosensing of Bacteria and Bacterial Communities. Journal of Analysis and Testing, 2017, 1, 1.	5.1	21
79	LOCALIZED OPTICAL PHENOMENA AND THE CHARACTERIZATION OF MATERIALS INTERFACES. Annual Review of Materials Research, 1997, 27, 469-498.	5.5	20
80	Addressable Direct-Write Nanoscale Filament Formation and Dissolution by Nanoparticle-Mediated Bipolar Electrochemistry. ACS Nano, 2017, 11, 4976-4984.	14.6	20
81	Ion Gating in Nanopore Electrode Arrays with Hierarchically Organized pH-Responsive Block Copolymer Membranes. ACS Applied Materials & Interfaces, 2020, 12, 55116-55124.	8.0	20
82	Electrokinetically driven fluidic transport in integrated three-dimensional microfluidic devices incorporating gold-coated nanocapillary array membranes. Lab on A Chip, 2008, 8, 1625.	6.0	19
83	lonic transport in nanocapillary membrane systems. Journal of Nanoparticle Research, 2012, 14, 1.	1.9	19
84	Enzymatic activity of surface-immobilized horseradish peroxidase confined to micrometer- to nanometer-scale structures in nanocapillary array membranes. Analyst, The, 2009, 134, 851.	3.5	18
85	Electrokinetic control of fluid transport in gold-coated nanocapillary array membranes in hybrid nanofluidic–microfluidic devices. Lab on A Chip, 2010, 10, 1237.	6.0	18
86	Nanopore-enabled electrode arrays and ensembles. Mikrochimica Acta, 2016, 183, 1019-1032.	5.0	18
87	Whole-cell biosensing by siderophore-based molecular recognition and localized surface plasmon resonance. Analytical Methods, 2019, 11, 296-302.	2.7	18
88	Conductance-Based Chemical Sensing in Metallic Nanowires and Metal-Semiconductor Nanostructures. Analytical Chemistry, 2012, 84, 2-8.	6.5	17
89	Nanochannel Arrays for Molecular Sieving and Electrochemical Analysis by Nanosphere Lithography Templated Graphoepitaxy of Block Copolymers. ACS Applied Materials & Interfaces, 2017, 9, 24908-24916.	8.0	17
90	Voltageâ€Gated Nanoparticle Transport and Collisions in Attoliterâ€Volume Nanopore Electrode Arrays. Small, 2018, 14, e1703248.	10.0	17

#	Article	IF	CITATIONS
91	Electrochemical Immunosensing of Interleukin-6 in Human Cerebrospinal Fluid and Human Serum as an Early Biomarker for Traumatic Brain Injury. ACS Measurement Science Au, 2021, 1, 65-73.	4.4	17
92	Functional-DNA–Based Nanoscale Materials and Devices for Sensing Trace Contaminants in Water. MRS Bulletin, 2008, 33, 34-41.	3.5	16
93	Electrochemical Control of Stability and Restructuring Dynamics in Auâ^'Agâ^'Au and Auâ^'Cuâ^'Au Bimetallic Atom-Scale Junctions. ACS Nano, 2010, 4, 2946-2954.	14.6	16
94	Nanoporous Ag–GaN thin films prepared by metalâ€assisted electroless etching and deposition as threeâ€dimensional substrates for surfaceâ€enhanced Raman scattering. Journal of Raman Spectroscopy, 2012, 43, 1347-1353.	2.5	16
95	Capture of Single Silver Nanoparticles in Nanopore Arrays Detected by Simultaneous Amperometry and Surface-Enhanced Raman Scattering. Analytical Chemistry, 2019, 91, 4568-4576.	6.5	16
96	Fluidic communication between multiple vertically segregated microfluidic channels connected by nanocapillary array membranes. Electrophoresis, 2008, 29, 1237-1244.	2.4	15
97	Tunable electrochemical pH modulation in a microchannel monitored via the proton-coupled electro-oxidation of hydroquinone. Biomicrofluidics, 2014, 8, 044120.	2.4	15
98	Stable Atom-Scale Junctions on Silicon Fabricated by Kinetically Controlled Electrochemical Deposition and Dissolution. ACS Nano, 2008, 2, 1581-1588.	14.6	14
99	Spatiotemporal Distribution of Pseudomonas aeruginosa Alkyl Quinolones under Metabolic and Competitive Stress. MSphere, 2020, 5, .	2.9	14
100	Convective Delivery of Electroactive Species to Annular Nanoband Electrodes Embedded in Nanocapillaryâ€Array Membranes. Small, 2013, 9, 90-97.	10.0	13
101	Redox Cycling in Individually Encapsulated Attoliter-Volume Nanopores. ACS Nano, 2018, 12, 12923-12931.	14.6	13
102	Chemical Noise Produced by Equilibrium Adsorption/Desorption of Surface Pyridine at Au–Ag–Au Bimetallic Atom-Scale Junctions Studied by Fluctuation Spectroscopy. Journal of the American Chemical Society, 2013, 135, 4522-4528.	13.7	12
103	Non-aqueous microchip electrophoresis for characterization of lipid biomarkers. Interface Focus, 2013, 3, 20120096.	3.0	12
104	Label-free molecular imaging of bacterial communities of the opportunistic pathogen Pseudomonas aeruginosa. , 2016, 9930, .		12
105	On-demand in situ generation of oxygen in a nanofluidic embedded planar microband electrochemical reactor. Microfluidics and Nanofluidics, 2015, 19, 1181-1189.	2.2	10
106	Redox cycling-based detection of phenazine metabolites secreted from <i>Pseudomonas aeruginosa</i> in nanopore electrode arrays. Analyst, The, 2021, 146, 1346-1354.	3.5	10
107	Electrochemical and spectroelectrochemical characterization of bacteria and bacterial systems. Analyst, The, 2021, 147, 22-34.	3.5	10
108	Coupled Electrokinetic Transport and Electron Transfer at Annular Nanoband Electrodes Embedded in Cylindrical Nanopores. ChemElectroChem, 2014, 1, 1570-1576.	3.4	9

#	Article	IF	CITATIONS
109	Electric field effects on current–voltage relationships in microfluidic channels presenting multiple working electrodes in the weak-coupling limit. Microfluidics and Nanofluidics, 2015, 18, 131-140.	2.2	9
110	Acid–base chemistry at the single ion limit. Chemical Science, 2020, 11, 10951-10958.	7.4	9
111	Tunable optical metamaterial-based sensors enabled by closed bipolar electrochemistry. Analyst, The, 2019, 144, 6240-6246.	3.5	8
112	Electrowettingâ€Mediated Transport to Produce Electrochemical Transistor Action in Nanopore Electrode Arrays. Small, 2020, 16, e1907249.	10.0	8
113	Electrochemical Zero-Mode Waveguide Potential-Dependent Fluorescence of Glutathione Reductase at Single-Molecule Occupancy. Analytical Chemistry, 2022, 94, 3970-3977.	6.5	8
114	Robust Au–Ag–Au Bimetallic Atom-Scale Junctions Fabricated by Self-Limited Ag Electrodeposition at Au Nanogaps. ACS Nano, 2011, 5, 8434-8441.	14.6	7
115	In Situ Probing of Laser Annealing of Plasmonic Substrates with Surface-Enhanced Raman Spectroscopy. Journal of Physical Chemistry C, 2018, 122, 11031-11037.	3.1	7
116	Surface-Growing Communities of Pseudomonas aeruginosa Exhibit Distinct Alkyl Quinolone Signatures. Microbiology Insights, 2018, 11, 117863611881773.	2.0	7
117	Perturbation of Microfluidic Transport Following Electrokinetic Injection through a Nanocapillary Array Membrane: Injection and Biphasic Recovery. Journal of Physical Chemistry C, 2008, 112, 19242-19247.	3.1	6
118	Effects of molecular confinement and crowding on horseradish peroxidase kinetics using a nanofluidic gradient mixer. Lab on A Chip, 2016, 16, 877-883.	6.0	5
119	Science and technology of electrochemistry at nano-interfaces: concluding remarks. Faraday Discussions, 2018, 210, 481-493.	3.2	5
120	Potential dependent spectroelectrochemistry of electrofluorogenic dyes on indiumâ€ŧin oxide. Electrochemical Science Advances, 2022, 2, e2100094.	2.8	5
121	Spatiotemporal dynamics of molecular messaging in bacterial co-cultures studied by multimodal chemical imaging. , 2019, 10863, .		5
122	Actively Controllable Solid-Phase Microextraction in a Hierarchically Organized Block Copolymer-Nanopore Electrode Array Sensor for Charge-Selective Detection of Bacterial Metabolites. Analytical Chemistry, 2021, 93, 14481-14488.	6.5	5
123	Potential-Dependent Restructuring and Chemical Noise at Au–Ag–Au Atomic Scale Junctions. ACS Nano, 2014, 8, 1718-1727.	14.6	4
124	From single cells to single molecules: general discussion. Faraday Discussions, 2016, 193, 141-170.	3.2	4
125	Directâ€Write Formation and Dissolution of Silver Nanofilaments in Ionic Liquidâ€Polymer Electrolyte Composites. Small, 2018, 14, 1802023.	10.0	4
126	Nanopore-Templated Silver Nanoparticle Arrays Photopolymerized in Zero-Mode Waveguides. Frontiers in Chemistry, 2019, 7, 216.	3.6	4

#	Article	IF	CITATIONS
127	Silver Nanofilament Formation Dynamics in a Polymerâ€lonic Liquid Thin Film by Direct Write. Advanced Functional Materials, 2020, 30, 1907950.	14.9	4
128	Biopolymer Patterning-Directed Secretion in Mucoid and Nonmucoid Strains of <i>Pseudomonas aeruginosa</i> Revealed by Multimodal Chemical Imaging. ACS Infectious Diseases, 2021, 7, 598-607.	3.8	4
129	Processes at nanopores and bio-nanointerfaces: general discussion. Faraday Discussions, 2018, 210, 145-171.	3.2	3
130	Depth distributions of signaling molecules in Pseudomonas aeruginosa biofilms mapped by confocal Raman microscopy. Journal of Chemical Physics, 2021, 154, 204201.	3.0	3
131	Microchannel Voltammetry in the Presence of Large External Voltages and Electric Fields. Analytical Chemistry, 2016, 88, 4200-4204.	6.5	2
132	Microscale and Nanoscale Electrophotonic Diagnostic Devices. Cold Spring Harbor Perspectives in Medicine, 2019, 9, a034249.	6.2	2
133	Potential-induced wetting and dewetting in pH-responsive block copolymer membranes for mass transport control. Faraday Discussions, 2021, 233, 283-294.	3.2	2
134	Coupling of 3D Porous Hosts for Li Metal Battery Anodes with Viscous Polymer Electrolytes. Journal of the Electrochemical Society, 2022, 169, 010511.	2.9	2
135	Potential-induced wetting and dewetting in hydrophobic nanochannels for mass transport control. Current Opinion in Electrochemistry, 2022, 34, 100980.	4.8	2
136	Using Raman spectroscopy and SERS for in situ studies of rhizosphere bacteria. , 2015, 9550, .		1
137	Ionic transport in nanocapillary membrane systems. , 2012, , 17-31.		0
138	Nanofluidics: Convective Delivery of Electroactive Species to Annular Nanoband Electrodes Embedded in Nanocapillary-Array Membranes (Small 1/2013). Small, 2013, 9, 164-164.	10.0	0
139	Electrochemical Zero-Mode Waveguide Studies of Single Enzyme Reactions. , 2018, 2018, .		0
140	Emerging Directions in Electroanalysis. Journal of Analysis and Testing, 2019, 3, 123-124.	5.1	0
141	Nanopore-Organized Nanoparticle Arrays for Tunable Optical Materials Using Nanobioplar Electrodeposition. ECS Meeting Abstracts, 2018, , .	0.0	0
142	(Invited) Closed Bipolar Electrochemistry with Multiplex Optical Readout for Rapid Diagnostics of Sepsis Syndrome Biomarkers. ECS Meeting Abstracts, 2019, , .	0.0	0
143	Spatiotemporal distribution of chemical signatures exhibited by Myxococcus xanthus in response to metabolic conditions. Analytical and Bioanalytical Chemistry, 2022, 414, 1691-1698.	3.7	Ο